# Glioblastoma-derived Tumor Cells Induce Vasculogenic Mimicry through Flk-1 Protein Activation*[S]

Ralph Francescone[‡1], Steve Scully[‡1], Brooke Bentley[§], Wei Yan[§], Sherry L. Taylor[¶], Dennis Oh[¶], Luis Moral[||], and Rong Shao[‡§**2]

From the [‡]Molecular and Cellular Biology Program, Morrill Science Center, University of Massachusetts, Amherst, Massachusetts 01003, the [§]Pioneer Valley Life Sciences Institute, Springfield, Massachusetts 01199, the Departments of [¶]Neurosurgery and [||]Pathology, Baystate Medical Center, Tufts University, Springfield, Massachusetts 01199, and the [**]Department of Veterinary and Animal Sciences, University of Massachusetts, Amherst, Massachusetts 01003

**Background:** The malignancy of glioblastoma is characterized by strong vascularization, including vasculogenic mimicry and angiogenesis.
**Results:** Glioblastoma cells promote vasculogenic mimicry and tumor development via Flk-1 activation.
**Conclusion:** Glioblastoma cells display the ability to constitute vascular channels.
**Significance:** Identification of Flk-1 as a key factor regulating vasculogenic mimicry could offer a novel therapeutic target for patient treatment.

**Glioblastoma (GBM) is extremely aggressive and essentially incurable. Its malignancy is characterized by vigorous microvascular proliferations. Recent evidence has shown that tumor cells display the ability to drive blood-perfused vasculogenic mimicry (VM), an alternative microvascular circulation independent of endothelial cell angiogenesis. However, molecular mechanisms underlying this vascular pathogenesis are poorly understood. Here, we found that vascular channels of VM in GBM were composed of mural-like tumor cells that strongly express VEGF receptor 2 (Flk-1). To explore a potential role of Flk-1 in the vasculogenesis, we investigated two glioblastoma cell lines U87 and GSDC, both of which express Flk-1 and exhibit a vascular phenotype on Matrigel. Treatment of both cell lines with either *Flk-1* gene knockdown or Flk-1 kinase inhibitor SU1498 abrogated Flk-1 activity and impaired vascular function. Furthermore, inhibition of Flk-1 activity suppressed intracellular signaling cascades, including focal adhesion kinase and mitogen-activated protein kinase ERK1/2. In contrast, blockade of VEGF activity by the neutralizing antibody Bevacizumab failed to recapitulate the impact of SU1498, suggesting that Flk-1-mediated VM is independent of VEGF. Xenotransplantation of SCID/Beige mice with U87 cells and GSDCs gave rise to tumors harboring robust mural cell-associated vascular channels. *Flk-1* shRNA restrained VM in tumors and subsequently inhibited tumor development. Collectively, all the data demonstrate a central role of Flk-1 in the formation of VM in GBM. This study has shed light on molecular mechanisms mediating tumor aggressiveness and also provided a therapeutic target for patient treatment.**

Glioblastoma (GBM)[3] is an extremely aggressive brain tumor with a median survival of ~12 months, irrespective of surgical resection and post-operative adjuvant radio/chemotherapy (1). More than 70% of patients with GBM succumb to the disease in 2 years, and fewer than 10% are alive 5 years following the initial diagnosis (2). The aggressiveness of this disease is characterized by strong vascular proliferation that is highly correlated with the malignancy of GBM. Thus, most of the current chemotherapies against GBM aim at vascular endothelial cells that orchestrate a significant component of blood vessels (3). However, it has been increasingly documented that an anti-angiogenic monotherapy did not give rise to a promise for improvement of patient overall survival, as drug resistance or angiogenic rebound occurs once the treatment is terminated (4, 5). For example, clinical trials using a neutralizing anti-VEGF antibody (Bevacizumab, also named Avastin) in recurrent GBMs revealed minimal benefit to patient survival (4, 6, 7). Consistent with clinical evidence, the anti-angiogenic preclinical studies using animal models reported conflicting outcomes in which malignant tumors unexpectedly developed (8, 9), implicating that escape mechanisms may account for the malignancy.

Recently, a number of research groups have demonstrated that vasculogenic mimicry (VM), an alternative vascular mechanism, contributes a central role to the vascularization of GBM in which tumor cells participate (10–12). Growing evidence suggests that this matrix-embedded, blood-perfused microvasculature renders tumor progression independent of endothelial cell angiogenesis (13, 14). In addition, this VM is believed to be at least partially ascribed to the multipotency of glioblastoma stem cells (GSCs) capable of transdifferentiation into vascular nonendothelial cells (15, 16). Furthermore, these studies suggest that transdifferentiation of GSCs into mural-like tumor

---

[3] The abbreviations used are: GBM, glioblastoma; VM, vasculogenic mimicry; Flk-1, VEGF receptor 2; Sma, smooth muscle α-actin; HMVEC, human microvascular endothelial cells; FAK, focal adhesion kinase; IHC, immunohistochemistry; PDGFR, platelet-derived growth factor receptor; PAS, periodic acid-Schiff; GSC, glioblastoma stem cell; h, human; cad, cadherin.

cells enables these vascular cells to constitute blood-perfused channels, whereas endothelial cells induce angiogenesis in GBM.

An angiogenic factor VEGF is appreciated to evoke vascular endothelial cell angiogenesis mainly through binding its membrane-bound receptors such as VEGF receptor 1/Flt-1 and VEGF receptor 2/Fms-like tyrosine kinase-1 or kinase domain receptor (Flk-1/KDR) (17, 18). Flk-1 is the earliest differentiation marker for endothelial cells and blood cells (19, 20). Expression of Flk-1 in the adult is restricted to endothelial cells and is transiently up-regulated during angiogenesis (17). Deletion of the *Flk-1* gene in mice results in embryonic lethality because of the lack of hematopoietic and endothelial lineage development (20, 21). Once binding with VEGF, Flk-1 undergoes autophosphorylation of tyrosine residues located in an intracellular kinase domain and it subsequently activates multiple intracellular signaling cascades such as focal adhesion kinase (FAK) and MAPK activation, leading to endothelial cell angiogenesis (*e.g.* cell proliferation, migration, and tube formation) (22, 23). Interestingly, previous studies showed that transdifferentiation of embryonic stem cells into vascular endothelial cells and mural cells required expression of Flk-1 (24–26). However, it is largely unknown whether Flk-1 plays an essential role in the development of VM. Here, we take advantage of GBM-derived tumor cell lines capable of developing VM to investigate a role of Flk-1 in the vasculogenesis of GBM. Deciphering the molecular mechanisms will offer considerable value for devising a novel therapeutic regimen targeting non-endothelial vascular proliferation in concert with current anti-angiogenic therapy.

## EXPERIMENTAL PROCEDURES

*Cell Culture*—U87 cells were purchased from the ATCC. GSDCs were established from a tumor sample of a patient with GBM after the study was approved by Baystate Medical Center Institutional Review Board. Briefly, a small fragment of a tumor sample was digested with an enzymatic mixture containing 1.3 mg/ml trypsin (Sigma), 0.67 mg/ml type 1-S hyaluronidase (Sigma), and 0.13 mg/ml kynurenic acid (Sigma). Following extensive washing, cells were resuspended and cultured in DMEM/F-12 supplemented with B27 (Invitrogen) and 20 ng/ml bFGF and EGF for 2 weeks. Then the cells were transferred to a new plate and grown in DMEM supplemented with 10% FBS as the same medium used for U87 cells. GSDCs at passages between 10 and 20 were used for the study. Human microvascular endothelial cells (HMVECs) established previously were grown in a medium from the EBM2 kit supplemented with hydrocortisone, EGF, and 10% FBS (Lonza Inc, Allendale, NJ) (27).

*Tube Formation*—Tube formation was performed as described previously (28). In brief, cells were plated on growth factor-reduced Matrigel (10 mg/ml, BD Biosciences) overnight, and tubules were fixed with 10% formalin and imaged followed by quantification. Density of tubules was quantified from random selection of three fields under a microscope.

*Flk-1 Gene Knockdown*—A PGPU6-GFP-neo shRNA expression vector containing DNA oligonucleotides (21 bp) (GenePharma, Shanghai, China) specifically targeting the C

terminus (5′-GCTTGGCCCGGGATATTTATA-3′) of *Flk-1* or the vector with non-sense oligonucleotides as a control was transfected into U87 cells using FuGENE 6. Cells were selected in 800 $\mu$g/ml G418 starting 48 h after transfection, and GFP expression was monitored to evaluate transfection efficiency.

*Immunoprecipitation and Immunoblotting*—Cell lysates were processed as described previously (29). The lysates were then incubated with an anti-pY20 antibody (ICN Biomedicals, Aurora, OH) at 4 °C overnight followed by incubation with protein A-Sepharose beads at 4 °C for 4 h. The immunocomplex was extensively washed, and the samples were run on SDS-PAGE. Then proteins were transferred to a PVDF membrane (VWR, Rockford, IL) and incubated with an anti-Flk-1 monoclonal antibody (Santa Cruz Biotechnology, Inc., Santa Cruz, CA) or anti-FAK polyclonal antibody (BIOSOURCE). Membranes were then incubated with a goat anti-mouse secondary antibody (The Jackson Laboratory). Specific signals were detected by enhanced chemiluminescence (VWR Scientific). For immunoblotting only, blot membranes were incubated with one of a series of primary antibodies against Flk-1, CD31, Tie1, Tie2 (Santa Cruz Biotechnology), SMa (Abcam, Cambridge, MA), VE-, N-cad (Invitrogen), FAK (BIOSOURCE), pERK1/2, ERK1/2 (Santa Cruz Biotechnology), or actin (Sigma).

*Immunocytochemistry*—Cells plated on 24-well plates were fixed with 4% paraformaldehyde and permeabilized with 0.5% Triton X-100 in PBS. The samples were incubated overnight with antibodies specific for Flk-1 (rabbit), VE-cad (mouse), and SMa (rabbit). Alexa Fluor 488 and 555 goat anti-mouse and -rabbit antibodies (Invitrogen) were added for 1 h followed by nuclear staining with 4′,6-diamidino-2-phenylindole (DAPI) (Invitrogen).

*Live/Dead Assay*—Live/Dead Assay kit (Invitrogen) was employed to determine living *versus* dead cells as instructed by the manufacturer. Briefly, living cells were stained with 2 $\mu$M calcein AM (green), and dead cells were stained with 4 $\mu$M ethidium homodimer (red) for 30 min. Cells were then imaged, and live/dead cells were quantified.

*Tumor Xenografts in Mice*—All animal experiments were performed with the approval of Institutional Animal Care and Use Committee of the University of Massachusetts and Baystate Medical Center. SCID/Beige mice were injected subcutaneously with U87 cells ($8 \times 10^6$) or GSDCs ($5 \times 10^6$) in 0.2 ml of PBS. Tumors arising from injected cells were monitored weekly for 8 weeks, after which the animals were humanely sacrificed. Mice were examined for expression of GFP using the Maestro *in vivo* imaging system (CRI, Woburn, MA). The tumors were measured, and volume was calculated as follows: volume = length $\times$ width$^2 \times 0.52$.

*Immunohistochemistry and Immunofluorescence*—Paraffin-embedded or frozen tumor tissues were cut to 6 $\mu$m thickness and processed for immunohistochemical analysis. In brief, samples were incubated with 3% $H_2O_2$ for 30 min to block endogenous peroxidase activity, followed by incubation with blocking buffer containing 10% goat serum for 1 h. The samples then were incubated at room temperature for 2 h with mouse anti-Flk-1 (1:200) (Santa Cruz Biotechnology), anti-hCD31 (1:100), anti-hCD34 (1:200), anti-SMa (1:500) (Dako Inc., Car-
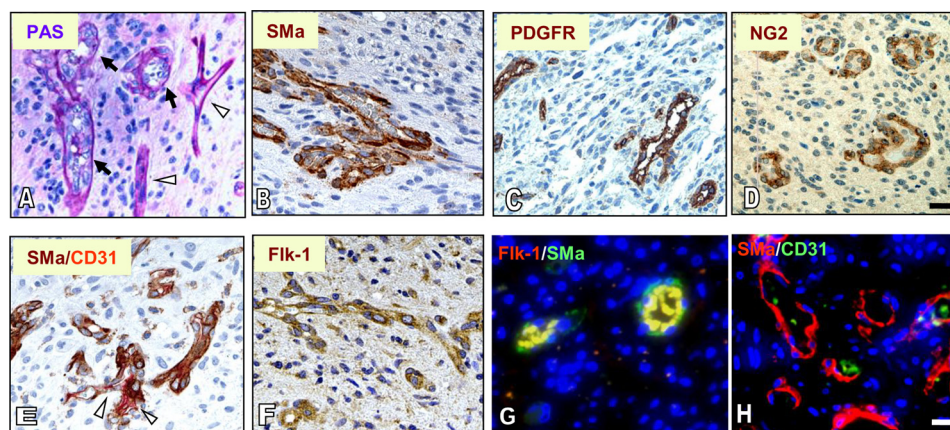
FIGURE 1. **Extensive tumor cell-associated, blood-perfused channels co-express SMa, PDGFR, and Flk-1 in GBMs.** Tumor specimens were subjected to staining of PAS (*A*), IHC of SMa (*B*), PDGFR (*C*), NG2 (*D*), SMa and CD31 (*E*), Flk-1 (*F*), and immunofluorescent co-staining of SMa with Flk-1 (*G*) and SMa with CD31 (*H*). *A, arrows* represent tumor cell-associated vascular channels in which blood cells are located (thick vessel walls), and *arrowheads* indicate endothelial cell-associated vessels (thin vessel walls). *E, arrowhead* indicates CD31-positive vessels. *G*, vessels were strongly positive for Flk-1 and Sma; *H*, a few vessels expressed CD31. *Bars*, 100 $\mu$m.

pentaria, CA), rat anti-mCD31 (1:50, BD Biosciences) monoclonal antibodies, or rabbit anti-PDGFR (Santa Cruz Biotechnology), and anti-GFAP (1:5000, Dako) polyclonal antibodies. Goat anti-mouse or anti-rabbit secondary antibodies (1:100) conjugated to HRP were added for 1 h. Finally, 3,3′-diaminobenzidine substrate (Dako) was introduced for several minutes, and after washing, methyl green or PAS was used for counterstaining. Dual immunohistochemistry labeling was performed using one primary antibody at 4 °C overnight followed by application of the secondary antibody conjugated to alkaline phosphatase and incubated with permanent red as a substrate (G2 kit, Dako). After extensive washing with TBST, the samples were then incubated with another primary antibody at room temperature for 2 h followed by application of a secondary antibody conjugated to HRP. Finally, 3,3′-diaminobenzidine substrate and counterstaining were performed as described above.

*Vasculature Quantification*—Three to five specimens randomly cut from each tumor block were processed for the IHC staining. Following the double staining with SMa and CD31, each sample was subjected to quantification of all the vessels that were positively stained for SMa, CD31, or both SMa and CD31 and that were negative staining but contained blood cells in the lumens. ImageJ software (National Institutes of Health) was used to quantify vessel density.

For dual immunofluorescent staining, tumor specimens were incubated with a mouse anti-hCD31 or Flk-1 for 2 h followed by incubation with a goat anti-mouse Alexa Fluor secondary antibody (1:250) for 1 h. Then the samples were similarly incubated with a rabbit anti-SMa or GFAP antibody followed by incubation with a goat anti-rabbit Alexa Fluor antibody. Finally, DAPI was added to stain nuclei.

*Statistics*—Data are expressed as mean ± S.E., and *n* refers to the numbers of individual experiments performed. Differences among groups were determined using one-way analysis of variance followed by the Newman-Keuls test. The 0.05 level of probability was used as the criterion of significance.

## RESULTS

To determine whether VM is present in GBM, we examined tumor samples from 11 patients with GBM. Hematoxylin and

eosin (H&E) showed a vascular pattern spread throughout the majority of the tumor sections in 7 of 11 tumors, and PAS staining of vascular basement membrane revealed extensive blood-perfused channels, most of which harbored vascular cells that displayed a torturous phenotype dissimilar to endothelial cells (Fig. 1, *A* and *B*). Two of the other tumors contained a minimal level of vascular channels, whereas the final two were avascular. To determine whether these vascular channels are composed of mural cells, we utilized an IHC approach by staining the samples with smooth muscle $\alpha$-actin (SMa) and PDGFR, both of which are vascular pericyte markers. A number of these vessels exhibited strong staining of both SMa and PDGFR (Fig. 1, *C* and *D*). In a dual staining analysis of SMa and CD31, a vascular endothelial cell marker, we found that some vessels contained endothelial cells and others consisted of SMa-positive cells (Fig. 1*E*). In addition, IHC analysis indicated that these mural cell-associated vessels were positive for Flk-1 (Fig. 1*F*). To validate that these mural-like tumor cells express Flk-1, we performed a dual immunofluorescent assay and found that a significant component of the vascular channels co-expressed SMa with Flk-1 (Fig. 1*G*) but not with CD31 (Fig. 1*H*). These data demonstrate that VM present in GBM is principally composed of mural cells that express Flk-1.

To test our hypothesis that tumor cells act as vascular mural-like cells to participate in VM, we investigated two glioblastoma tumor cell lines as follows: U87 cells and GSDCs that were established from patients with GBM. We performed immunoblotting to assess expression of mural and endothelial cell markers. Both tumor lines U87 and GSDCs expressed stronger Flk-1 than that observed in HMVECs (Fig. 2*A*). Contrary to HMVECs that express a barely detectable level of SMa, U87 cells and GSDCs expressed a higher level of SMa. Immunocytochemistry analysis unveiled the same expression pattern of Flk-1 and SMa as the immunoblotting results (Fig. 2, *A* and *B*). However, it was notable that both U87 cells and GSDCs, in contrast to HMVECs, did not express endothelial cell-specific markers VE-cad, CD31, Tie1, or Tie2, demonstrating that GSDCs are distinct from endothelial cells. U87 cells and GSDCs expressed higher N-cad than did HMVECs, consistent with
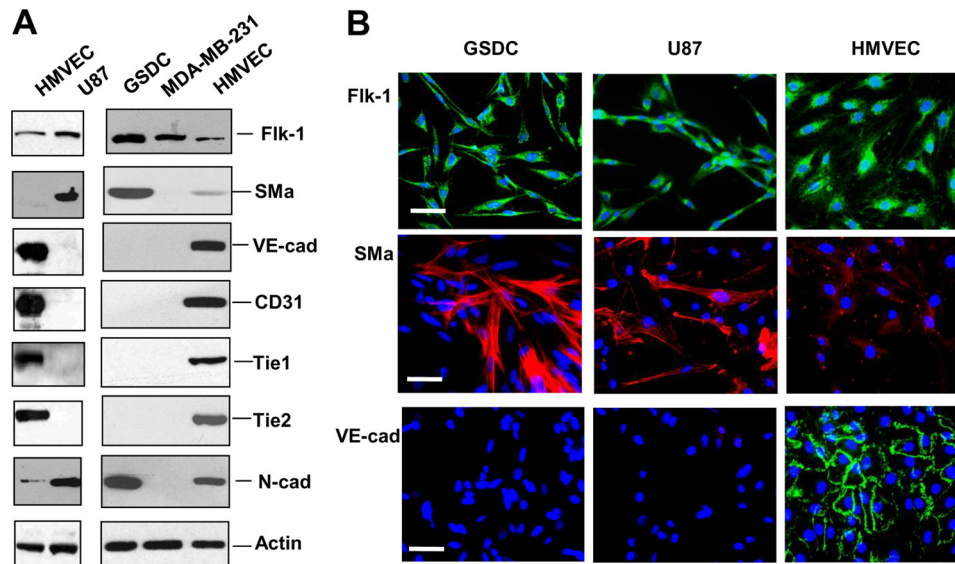
FIGURE 2. **U87 cells and GSDCs express SMa and Flk-1 but not endothelial cell markers.** *A,* cell lysates of U87 cells, GSDCs, MDA-MB-231 cells, and HMVECs were analyzed by immunoblotting against Flk-1, SMa, VE-cad, CD31, Tie1, Tie2, N-cad, and actin. MDA-MB-231 cells were used as a negative control. *B,* these cells were also used for immunocytochemistry staining of SMa, Flk-1, and VE-cad. DAPI is nuclear staining. *Bars,* 50 μm.

previous reports that vascular endothelial cells also express N-cad in addition to VE-cad (30, 31). To confirm that this mural cell expression pattern was not just an artifact of one particular patient-derived cell line, a second patient-derived cell line, GSDC-2, was created. GSDC-2 also showed a nearly identical expression pattern as GSDCs (supplemental Fig. 1, *A and B*), suggesting that this mural marker expression is a common characteristic of GBM cells.

Should U87 cells and GSDCs truly represent cells capable of developing vascular channels, they might possess the vasculogenic activity as do endothelial cells (27, 28). To test this hypothesis, we performed a tube formation assay that commonly recapitulates the ability of endothelial cells to develop vasculature *in vitro*. U87 cells and GSDCs formed a capillary phenotype on Matrigel in a cell number-dependent manner (Fig. 3, *A and B*). To evaluate if this vascular event is dependent on Flk-1 as expressed by mural cells (Fig. 1) in GBM, we employed a Flk-1 kinase inhibitor SU1498. Treatment with SU1498 inhibited the ability of both cells to induce a capillary-like structure by ~72–80% relative to controls (Fig. 3, *C and D*). To provide additional genetic evidence that Flk-1 is important for vasculogenic function, we used an *Flk-1* shRNA gene knockdown approach. Suppression of *Flk-1* was associated with a corresponding reduction in SMa expression and tube formation as tubules were decreased by 80% of control tubules (Fig. 3*E*). These findings were also validated with the GSDC-2 cell line derived from another patient (supplemental Fig. 1*C*). In all the tube formation assays, treatment of either SU1498 or *Flk-1* gene knockdown did not result in cell growth arrest or cell death (supplemental Fig. 2).

Next, we determined whether this Flk-1-mediated vascular activity requires VEGF. We treated these tumor cells with the anti-VEGF-neutralizing antibody Bevacizumab in the tube formation. As tested earlier, both U87 cells and GSDCs decreased the ability to develop tubules in the presence of SU1498. In contrast, they did not display dysfunction of the vascular formation once Bevacizumab was added (Fig. 4*A* and supplemental Fig. 1*C*). Accordingly,

expression of SMa in these cells was reduced by SU1498 but not by Bevacizumab, indicative of a VEGF-independent event. Regardless of higher expression of VEGF by U87 cells and GSDCs than that by HMVECs, this vasculogenic capability of these tumor cells was distinct from the angiogenic signature of vascular endothelial cells that highly responded to Bevacizumab in the development of tubules (Fig. 4*C*).

To further validate that Flk-1-mediated vasculogenesis does not require VEGF, we stimulated U87 cells with VEGF in the tube formation assay. Exposure of both U87 control cells and the cells expressing *Flk-1* shRNA to VEGF did not alter vascular development, as VEGF neither enhanced vascularization in the control cells nor rescued the impaired capability of tube formation in *Flk-1* shRNA cells (Fig. 4*D*). These data support the notion that Flk-1-mediated VM is independent of VEGF.

We then sought to determine whether Flk-1 kinase activity plays a core role in signaling activation independent of VEGF. Both U87 cells and GSDCs were treated with either SU1498 or Bevacizumab overnight (Fig. 5*A*). Consistent with earlier functional analyses, treatment of these cells with SU1498 resulted in 80–86% reduction of tyrosine-phosphorylated Flk-1 compared with control levels (Fig. 5, *A and B*). In contrast, Bevacizumab failed to alter pFlk-1 levels. To further identify intracellular signaling pathways in response to Flk-1 activation, we focused on FAK and downstream effector MAPK ERK1/2, as these intracellular factors mediate Flk-1 signaling in vascular endothelial cells (24, 29). We measured tyrosine-phosphorylated FAK and ERK1/2 after treatment of U87 cells and GSDCs with Bevacizumab and SU1498, and we found that activated levels of pFAK in SU1498-treated cells were reduced by ~50–75% relative to control or Bevacizumab-treated cells (Fig. 5, *A and B*). Accordingly, pERK1/2 were significantly decreased in SU1498 but not Bevacizumab-treated cells. As a result, SU1498 treatment led to suppression of SMa expression by 67–75% compared with the level in control or Bevacizumab-treated cells. All the data demonstrate that Flk-1 activation in tumor cells leads to intracellu-
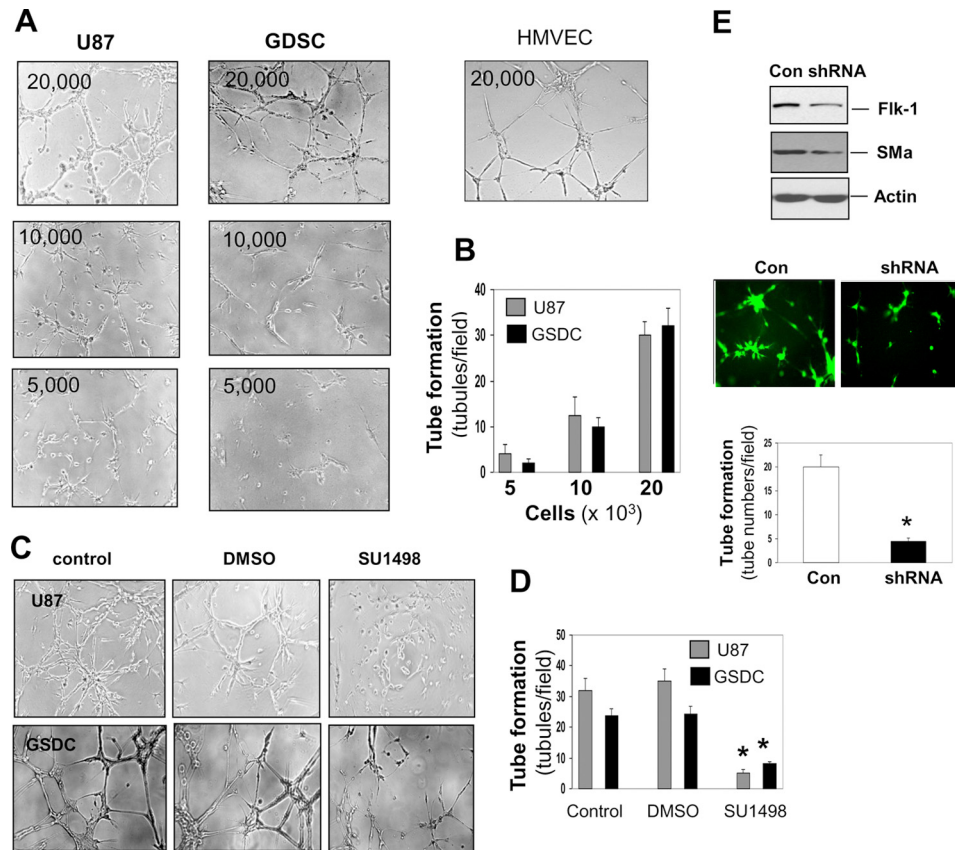
FIGURE 3. **U87 cells and GSDCs are able to induce vascular tube formation, the process dependent on Flk-1.** *A,* different cell numbers of U87 cells and GSDCs were cultured on Matrigel for tube formation. HMVECs served as a positive control. $n = 3$. *B,* tubules formed by these cells were quantified, demonstrating a cell number-dependent relationship. *C,* tube formation was performed overnight with U87 cells and GSDCs ($2 \times 10^4$) in the presence of SU1498 (12.5 $\mu$M). *D,* tubules were quantified. $n = 4$. *, $p < 0.05$ compared with controls or DMSO treatment. *E,* U87 cells were used to knock down the *Flk-1* gene. Cell lysates were collected for detection of Flk-1, SMa, and actin by immunoblotting. Cells carrying scrambled RNA GFP vector or sh*Flk-1* RNA GFP vector were analyzed for tube formation under a fluorescence microscope followed by quantification. $n = 3$. *, $p < 0.05$ compared with a control (*con*).
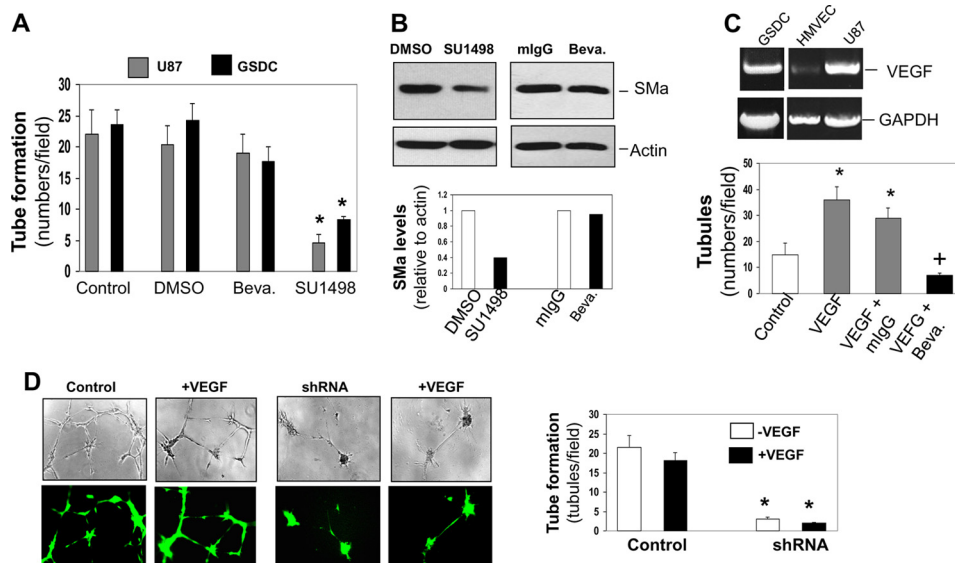


FIGURE 4. **Flk-1-mediated vasculogenesis is independent of VEGF.** *A,* U87 cells and GSDCs were used for tube formation in the presence of an anti-VEGF antibody (Bevacizumab, *Beva.*) (10 $\mu$g/ml) or SU1498 (12.5 $\mu$M). Tubules were quantified. $n = 4$. *, $p < 0.05$ compared with controls or DMSO treatment. *B,* U87 cells were treated with Bevacizumab (*Beva*) (10 $\mu$g/ml) or SU1498 (12.5 $\mu$M) for 24 h, and cell lysates were subjected to immunoblotting against SMa and actin followed by quantification. *C,* HMVECs were stimulated with VEGF (10 ng/ml) on Matrigel in the presence of Bevacizumab (10 $\mu$g/ml). Data were quantified. $n = 4$. *, +, $p < 0.05$ compared with control and VEGF + mIgG, respectively. *D,* U87 cells expressing non-sense RNA or *Flk-1* shRNA GFP vector were subjected to tube formation in the presence of VEGF (10 ng/ml). Tubules were imaged with a phase contrast and fluorescent microscope. $n = 3$. Data were quantified. *, $p < 0.05$ compared with corresponding control cells bearing scrambled RNA.
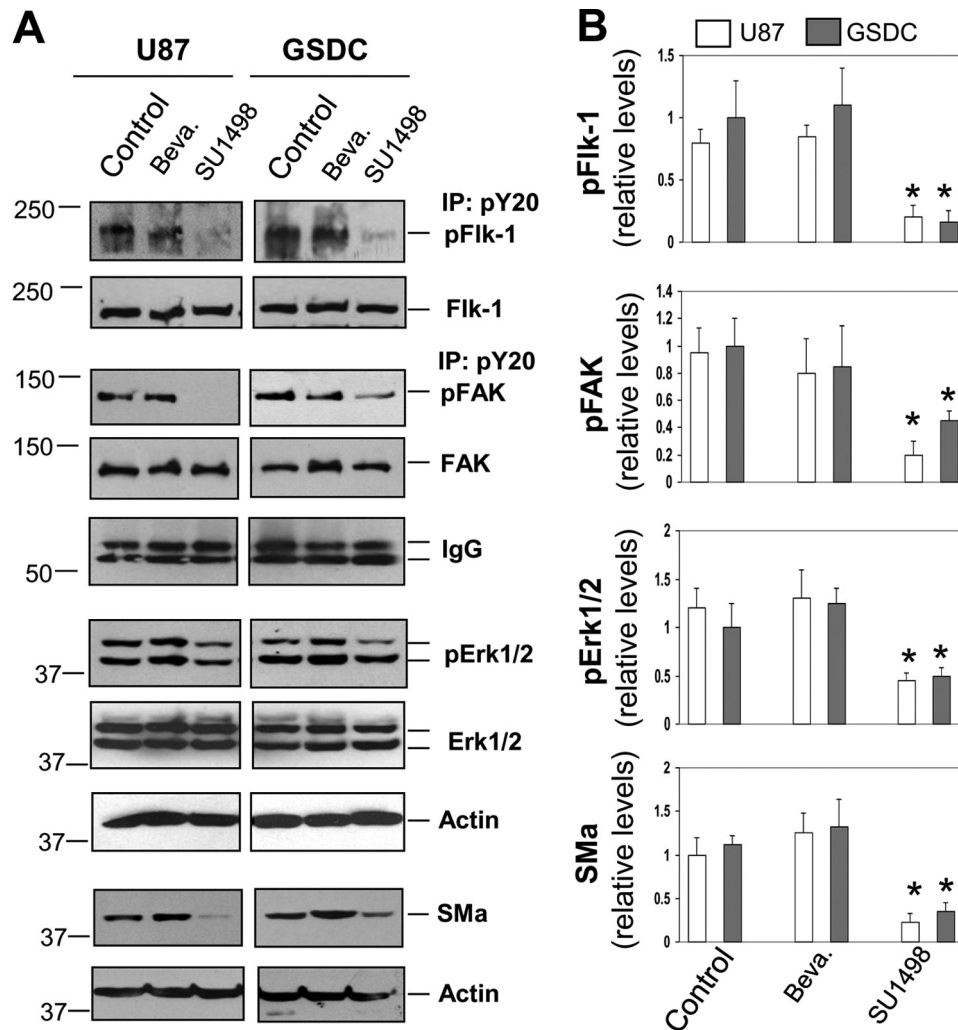
FIGURE 5. **Flk-1-mediated intracellular signaling activation is independent of VEGF.** *A*, U87 cells and GSDCs were treated with either Bevacizumab (*Beva*, 10 $\mu$g/ml) or SU1498 (12.5 $\mu$M) overnight and then collected for co-immunoprecipitation (*IP*) with an anti-pY20 antibody followed by immunoblotting with an anti-Flk-1 or FAK antibody. IgG of the anti-pY20 antibody was tested as loading controls. Some of these cell lysates were used for immunoblotting against Flk-1, FAK, pERK1/2, ERK1/2, and actin. In addition, some cells were treated with Bevacizumab (10 $\mu$g/ml) or SU1498 (12.5 $\mu$M) for 3 days, and the lysates were then measured for SMa expression. *B*, active forms of pFlk-1, pFAK, pERK1/2, and SMa were quantified by normalization with their corresponding total nonphosphorylated forms or actin. *n* = 3. *, *p* < 0.05 compared with corresponding control or Bevacizumab-treated groups.

lar signaling cascades FAK and ERK1/2 and SMa expression, but this event does not require VEGF stimulation.

To further confirm the intracellular signaling pathway mediating Flk-1 activation, we used a MAPK inhibitor, PD98059 (10 $\mu$M). Protein expression levels of both pERK1/2 and SMa were reduced by the inhibitor by 35 and 60% for U87 cells and 33 and 50% for GSDCs relative to the DMSO control (Fig. 6, *A* and *B*). Like Flk-1 inhibition, PD98059 reduced tube formation in both U87 and GSDC cells by 68 and 79% respectively (Fig. 6*C*). All the data support the notion that ERK1/2 participate in the vascular signaling pathway.

In an attempt to determine whether these GBM-derived tumor cell lines can develop VM *in vivo*, we utilized a tumor xenograft model by transplantation of GSDCs into SCID/Beige mice. Six of mice receiving GSDCs rapidly developed tumors in the 8-week period, and removed tumors were analyzed for tumor vasculogenesis. PAS staining revealed vigorous formation of vasculature in the tumors (Fig. 7*A*) reminiscent of its original vascular phenotype in GBM (Fig. 1*B*). These extensive

vascular channels expressed strong SMa (Fig. 7*B*), GFAP (Fig. 7*C*), and Flk-1 (Fig. 7*D*), in which blood cells were located. In addition, these tumor cell-derived vessels did not express mouse CD31 (Fig. 7, *E* and *F*), confirming that VM is divergent from endothelial cell angiogenesis. To test the possibility that GSDCs may undergo differentiation *in vivo* into endothelial cells that participate in angiogenesis, we employed different antibodies specific for recognizing human endothelial cells. Neither using an anti-human CD31 antibody nor an anti-CD34 antibody showed positive staining in the tissue (Fig. 7, *G* and *H*), which indicates the incapability of tumor cell transdifferentiation into endothelial cells. To validate that these Flk-1-positive vessels are derived from tumor cells and not from host endothelial cells, we employed a co-immunofluorescent assay in which GFAP and Flk-1 were stained with red and green fluorescence, respectively. Indeed, Flk-1-positive vascular channels co-expressed GFAP that is specific for glioblastoma cells (Fig. 7, *I–L*). Finally, to demonstrate that these GBM-lined VM channels were functional *in vivo*, we utilized primary GBM cells
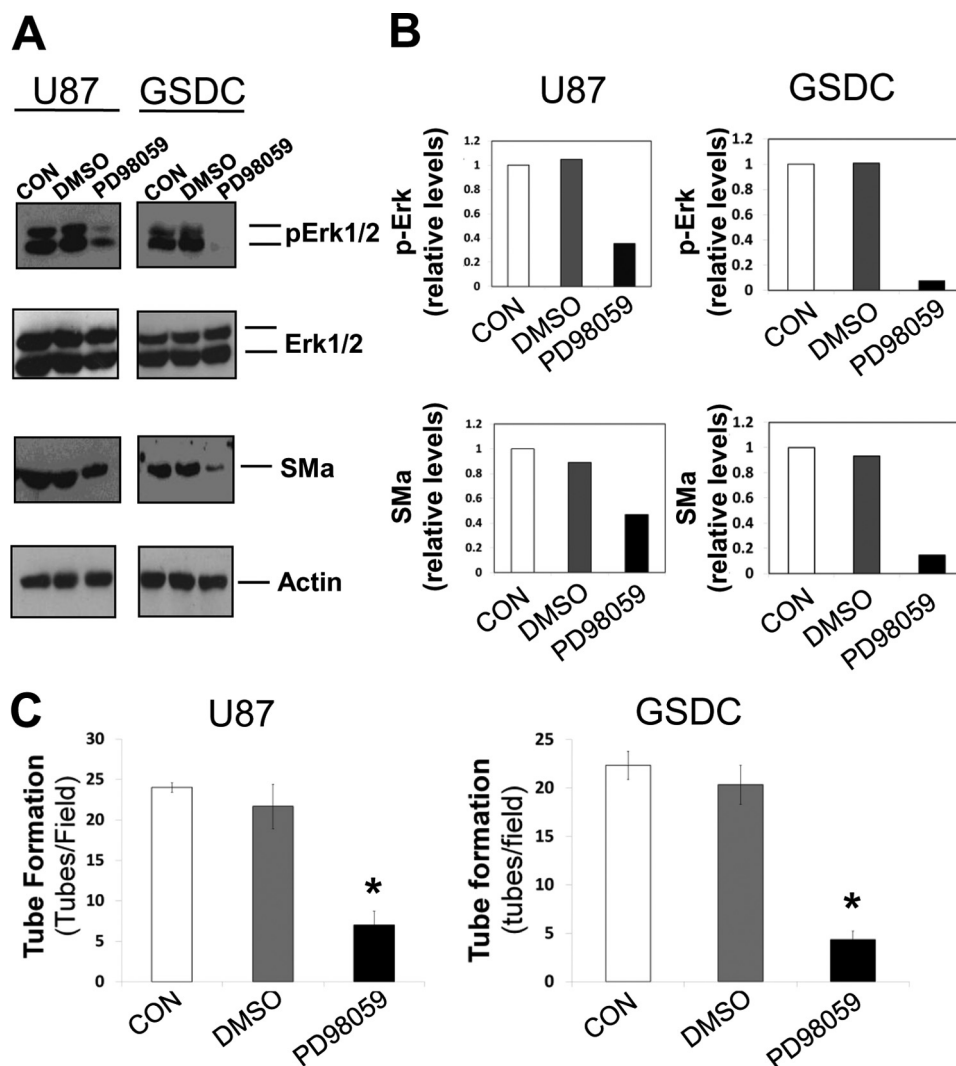
**A**

U87    GSDC

CON DMSO PD98059    CON DMSO PD98059

pErk1/2

Erk1/2

SMa

Actin

**B**

U87

GSDC

**C**

U87

GSDC

FIGURE 6. **Inhibition of downstream ERK signaling yields similar results to Flk-1 inhibition.** *A,* U87 or GSDC cells were either untreated (*CON*) or treated with DMSO or a MAPK inhibitor (PD98059, 10 $\mu$M) overnight, and lysates were collected. Immunoblotting of the lysates for ERK1/2, pERK1/2, SMa, and actin expression was performed. *B,* quantification of amounts of SMa and pERK1/2 shown in *A*. *C,* quantification of the functional analysis of the MAPK inhibitor on tube formation of either U87 or GSDC cells on Matrigel. $n = 3$, *, $p < 0.05$ compared with corresponding control groups.

expressing GFP, together with an intravenously injected fluorescent dye known as Evan's blue, 30 min prior to sacrificing (supplemental Fig. 3). Evan's blue was detected in the lumen of GFP$^+$ vessels, highlighting that these vascular channels are functional *in vivo*. These *in vivo* data suggest that transplanted glioblastoma cells participate in VM, rather than endothelial cell angiogenesis.

To establish a functional role for Flk-1 in the development of VM and tumor formation, we utilized another tumor xenograft model by transplantation of SCID/Beige mice with U87 cells expressing either control vector or *Flk-1* siRNA. All six animals receiving control U87 cells developed palpable tumors within 3 weeks, and all could be imaged for green fluorescence by week 8 (Fig. 8, *A* and *B*). In contrast, tumorigenesis was significantly delayed in mice receiving *Flk-1* shRNA-expressing U87 cells, and they did not develop palpable tumors until week 6. By weeks 6 and 8, these tumors were ~70% smaller than those observed in control counterparts, and the fluorescent images were undetectable during this period (Fig. 8, *A* and *B*). Postmortem histological analyses of tumors revealed that the control tumors harbored numerous tumor cell-derived channels, as demonstrated by extensive arbors of GFP-positive ramified channels throughout the entire tumor section (Fig. 8*C*), the event that resembled mural-like cell-lined channels identified in GBMs and above GSDC tumors (Figs. 1 and 7). In concert with earlier findings, the concomitant expression of PAS, SMa, and CD31 distinguished tumor cell-lined vasculature from endothelial cell vessels. SMa-positive vessels in control tumors were 7-fold greater than those found in shRNA tumors (Fig. 8, *C, panels c* and *d,* and *D*). Although SMa-positive channels were minimal in tumors expressing *Flk-1* shRNA, a significant fraction of vessels showed positive staining for mCD31, suggesting that endothelial cells orchestrate blood vessels in the absence of VM. In addition, IHC analysis using a single anti-hCD31 antibody revealed no detectable signal in either condition of tumors, consistent with earlier findings (Fig. 7, *G* and *H*). These results indicate lack of endothelial cell transdifferentiation from tumor cells. Collectively, all the *in vivo* data demonstrate that GBM cells promote VM, dependent on Flk-1, whereas host endothelial cells contribute to tumor angiogenesis.
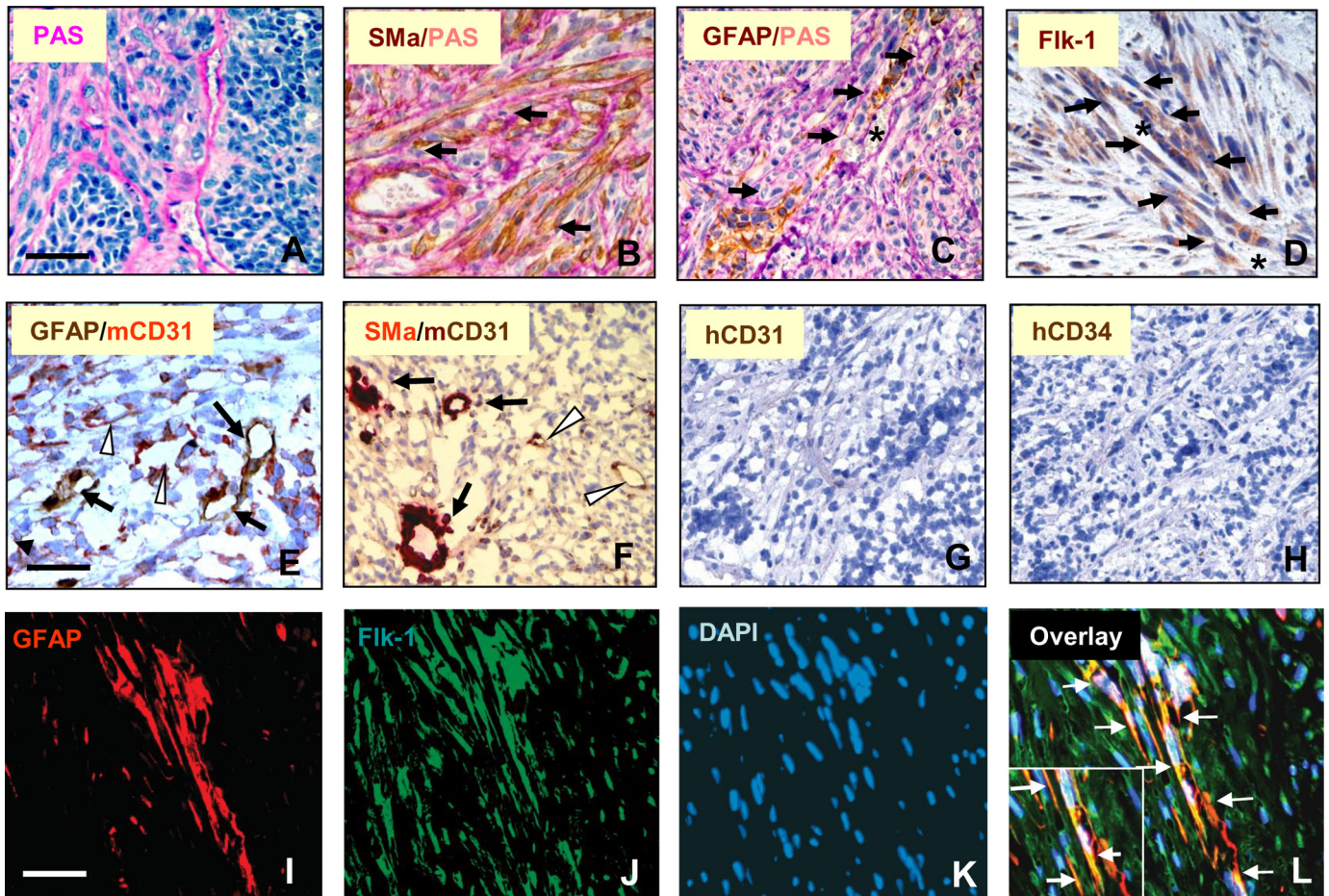
FIGURE 7. **GSDCs develop tumors that consist of tumor cell-associated vasculature co-expressing SMa, GFAP, and Flk-1.** Eight weeks following subcutaneous transplantation of GDSCs, tumors were removed and processed for IHC analysis of PAS (*A*), co-staining of SMa and PAS (*B*), GFAP and PAS (*C*), Flk-1 (*D*), GFAP and mCD31 (*E*), SMa and mCD31 (*F*), hCD31 (*G*), hCD34 (*H*), and co-immunofluorescent staining of GFAP (*I*), Flk-1 (*J*), and DAPI (*K*) in which an overlay image was displayed (*L*). *Black arrows* (*B–F*) indicate positive staining of VM vessel markers. *Asterisks* (*C* and *D*) specify the lumen of VM channels. *White arrowheads* (*E* and *F*) indicate positive staining of endothelial cell vessel markers. *White arrows* (*L*) indicate VM channels. *Inset* shows a large image for the channel. *Bars*, 100 $\mu$m.

## DISCUSSION

Tumor vasculature is traditionally assumed to arise from an endothelial cell origin (32). However, mounting evidence suggests that VM, the matrix-embedded, blood-perfused microvasculature, is an alternative mechanism for the development of tumor vessels, independent of endothelial cell angiogenesis (13, 14). For example, highly aggressive melanoma cells generate numerous matrix-rich patterned channels containing blood cells, and the formation of these channels positively correlates with the tumor malignancy (33, 34). A mosaic model consisting of both tumor cell- and endothelial cell-integrated networks was also described in the development of colon cancer (35, 36). Other recent reports suggest that mural-like tumor cells differentiated from GSCs promote VM (37–39). Consistent with these data, we identified that blood vessels of VM in GBM are composed of mural cell-lined vasculature, whereas endothelial cells contribute to angiogenesis, highlighting the different targets for clinical therapy. Furthermore, we demonstrate that tumor cell lines developed from GBM possess mural cell properties capable of forming vascular channels, and this vasculogenesis is dependent on Flk-1 activity.

VM has recently received considerable attention in the study of tumor development in the clinic, because a simplistic vasculature model focusing on endothelial cell angiogenesis merely is deemed insufficient to describe the entity of sophisticated neovascular networks in which tumor cells also participate (40, 41). For example, clinical trials of recurrent GBMs with Bevacizumab alone for inhibition of VEGF-induced angiogenesis did not result in significant improvement of disease survival (4, 6, 7). Thus, it is conceivable that the evasive responses may be at least in part attributed to VM. Indeed, our studies using Bevacizumab *in vitro* found that this Flk-1-mediated vascularization is VEGF-independent.

Flk-1 emerges as an essential angiogenic mediator to trigger signaling cascades induced by VEGF because of the expression of Flk-1 by endothelial cells. But this expression is not limited to endothelial cells only; instead, a number of nonendothelial cells, including stem cells and some tumor cells, also express Flk-1. For example, expression of Flk-1 acquired by embryonic stem cells confers differentiation into cardiac tissue and vascular cells such as endothelial cells and mural cells (24–26). Flk-1^{+}-neural stem cells have the potential to give rise to vascular
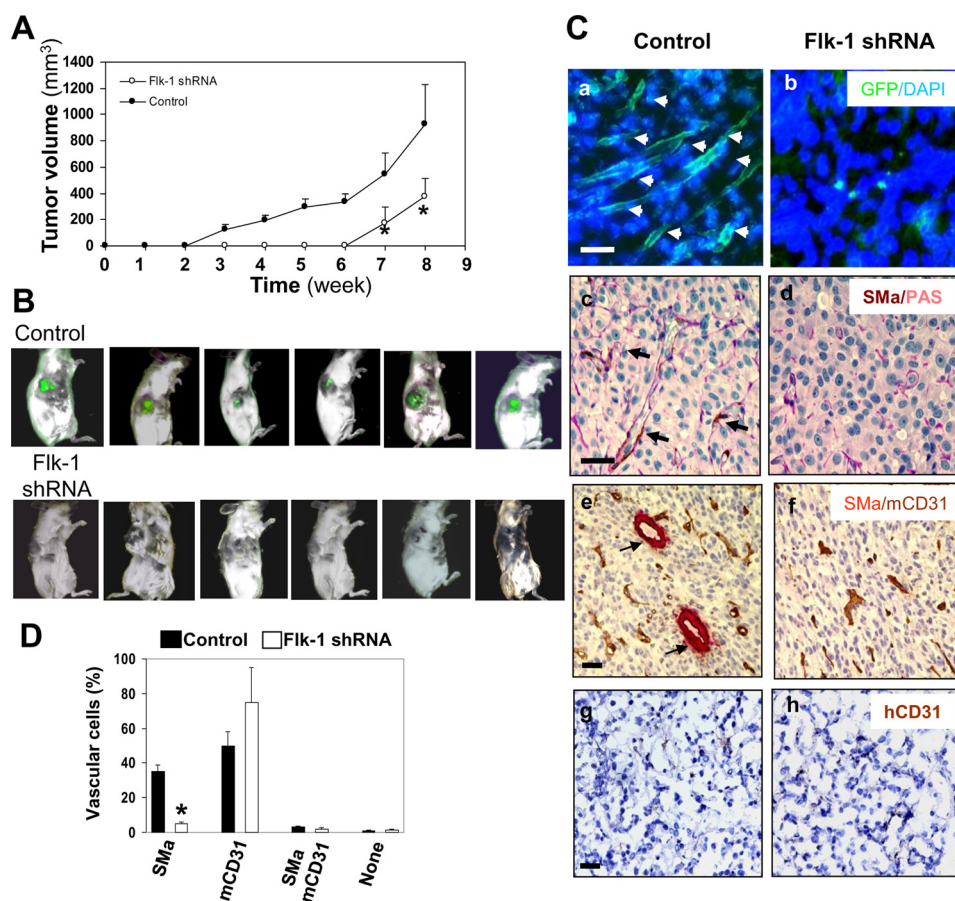
FIGURE 8. *Flk-1* shRNA in U87 cells inhibits tumor growth and VM. *A, Flk-1* gene knockdown results in suppression of tumor growth. U87 cells expressing *Flk-1* shRNA-GFP or GFP vector were injected subcutaneously into SCID/Beige mice, and tumor size was measured weekly for 8 weeks. $n = 6$. *, $p < 0.05$ compared with corresponding controls. *B*, tumor fluorescence was detectable only in mice injected with U87 cells expressing GFP vector. Before sacrifice, mice were examined for tumor fluorescence. Each image represented a single animal imaged 8 weeks after injection of the cells. *C*, formation of tumor cell-associated vascular channels was inhibited by *Flk-1* gene knockdown. Tumor fragments were examined for GFP fluorescence (*panels a* and *b*) and further analyzed by IHC for expression of co-staining of SMa with PAS (*panels c* and *d*), SMa with mCD31 (*panels e* and *f*), and a single staining of hCD31 (*panels g* and *h*). *Arrows* indicate GFP-positive (*panel a*) or SMa-positive tumor-cell-lined channels (*panels c* and *e*). *Bars,* 50 μm. *D,* quantification of vessels of VM and angiogenesis. Density of SMa and CD31-positive vessels present (*panels e* and *f*) was analyzed as described under "Experimental Procedures." $n = 6$. *, $p < 0.05$ compared with corresponding control tumors.

endothelial cells (42). In this study, we found that GBM-derived tumor cell lines express Flk-1 that controls VM in a VEGF-independent fashion. Furthermore, activation of Flk-1 triggers intracellular signaling cascades from FAK to MAPK ERK1/2, resembling angiogenic signaling in endothelial cells (24, 29). Although molecular mechanisms that regulate Flk-1 activation are currently still enigmatic in these cells, it is quite possible that it can be activated indirectly by other factors present in the tumor microenvironment such as extracellular matrix proteins. Most of these proteins (*e.g.* fibronectin) can bind to membrane-associated integrins and induce coordination of integrins with Flk-1, leading to Flk-1 activation (43–45). It is also possible that Flk-1 could be mutated to lose its binding affinity with VEGF or become constitutively active in the cells. Animal tumor models deficient of VEGF seem to be necessary to establish the notion that Flk-1 is an indispensable receptor tyrosine kinase independent of VEGF, which regulates mural cell-associated VM in GBM.

An anti-VEGF therapy with Bevacizumab was approved for the first-line treatment of a variety of advanced carcinomas, including brain tumor (3), breast cancer (46), colorectal cancer (47), and non-small-cell lung cancer (48, 49). However, the outcomes of this anti-angiogenic therapy in advanced tumors are still controversial. For instance, long term monotherapy with Bevacizumab in GBMs only receives transitory benefit without significantly prolonging survival (2, 50). Once the therapy stops, tumors undergo vascular recovery and rapidly regrow. Analogous to these clinical reports, evidence from animal studies using either anti-VEGF or VEGF receptor therapy shows opposite results, including blood revascularization, increased invasiveness, and distant metastasis (8, 51, 52). However, some interesting evidence from both clinical and preclinical trials using Flk-1 kinase inhibitors AZD2171, SU5416, or an anti-Flk-1 antibody show promising responses as these therapies ameliorate vascular normalization and alleviate peritumoral edema in GBMs and other cancers as well (53–57). In line with these data, our current findings have supported the hypothesis that VEGF and Flk-1 may independently regulate diverse vascularizations through divergent vascular cells in GBM. Therefore, the conjunct therapies against both VEGF and Flk-1 could be taken into account for the treatment of patients with GBM.

## Flk-1-mediated Vasculogenic Mimicry

Our animal models derived from both U87 cells and GSDCs exhibit extensive vascular channels formed by mural cells, recapitulating the vascular phenotype of GBM in which mural-like cell-associated vascular channels constitute a major component of vasculature. Interestingly, using an anti-human CD31 antibody failed to identify vessels positive for hCD31, demonstrating that tumor cells, unlike GSCs, are unable to undergo differentiation into endothelial cells. However, it is noteworthy that there is a significant population of mouse CD31-positive endothelial cells that are associated with tumor angiogenesis. This host-derived angiogenic response is plausibly ascribed to the accumulation of angiogenic factors secreted from the xenotransplanted tumor cells. Nevertheless, the mural cell-associated Flk-1-dependent VM, but not endothelial cell angiogenesis, plays an essential role in the tumor development.

It is also important to note that we used DMEM supplemented with 10% FBS to grow both the U87 cell line and the primary GBM cell line GSDC. In a separate study by Lee *et al.* (58), they demonstrated that the cancer cell lines grown in serum-free media supplemented with growth factors could cause cells to have a phenotype and genotype more indicative of primary tumors. Therefore, we cannot rule out a pheno/genotypic change in the U87s or GSDCs in the presence of serum. Nonetheless, the vascular phenotype *in vivo* of our cell lines resembles the observed vasculature in GBM patient tumors, indicating the VM mechanism represents the human condition to a certain extent.

In sum, our current findings provide mechanistic insights into the development of VM by tumor cells, the vascularization that occurs in a wide array of human cancers apart from GBM such as melanoma (13), breast cancer (59), prostate cancer (60), colorectal cancer (36), and ovarian cancer (61). Identification of Flk-1 as a key factor regulating VM could offer a novel therapeutic target for patient treatment. As a result, multiple anti-vascular approaches, including targeting VM and angiogenesis together with chemotherapy, may represent the best possible regimen in the fight against this devastating disease.

REFERENCES

1. Wen, P. Y., and Kesari, S. (2008) Malignant gliomas in adults. *N. Engl. J. Med.* **359,** 492–507
2. Norden, A. D., Drappatz, J., and Wen, P. Y. (2009) Antiangiogenic therapies for high grade glioma. *Nat. Rev. Neurosci.* **5,** 610–620
3. Nghiemphu, P. L., Liu, W., Lee, Y., Than, T., Graham, C., Lai, A., Green, R. M., Pope, W. B., Liau, L. M., Mischel, P. S., Nelson, S. F., Elashoff, R., and Cloughesy, T. F. (2009) Bevacizumab and chemotherapy for recurrent glioblastoma: a single-institution experience. *Neurology* **72,** 1217–1222
4. Bergers, G., and Hanahan, D. (2008) Modes of resistance to anti-angiogenic therapy. *Nat. Rev. Cancer* **8,** 592–603
5. Ellis, L.M., and Hicklin, D.J. (2008) VEGF-targeted therapy: mechanisms of anti-tumor activity. *Nat. Rev. Cancer* **8,** 579–591
6. Verhoeff, J. J., van Tellingen, O., Claes, A., Stalpers, L. J., van Linde, M. E., Richel, D. J., Leenders, W. P., and van Furth, W. R. (2009) Concerns about anti-angiogenic treatment in patients with glioblastoma multiforme. *BMC Cancer* **9,** 444
7. Kreisl, T. N., Kim, L., Moore, K., Duic, P., Royce, C., Stroud, I., Garren, N., Mackey, M., Butman, J. A., Camphausen, K., Park, J., Albert, P. S., and Fine, H. A. (2009) Phase II trial of single-agent bevacizumab followed by bevacizumab plus irinotecan at tumor progression in recurrent glioblastoma. *J. Clin. Oncol.* **27,** 740–745
8. Ebos, J. M., Lee, C. R., Cruz-Munoz, W., Bjarnason, G. A., Christensen, J. G., and Kerbel, R. S. (2009) Accelerated metastasis after short term treatment with a potent inhibitor of tumor angiogenesis. See comment. *Cancer Cell* **15,** 232–239
9. Pàez-Ribes, M., Allen, E., Hudock, J., Takeda, T., Okuyama, H., Viñals, F., Inoue, M., Bergers, G., Hanahan, D., and Casanovas, O. (2009) Antiangiogenic therapy elicits malignant progression of tumors to increased local invasion and distant metastasis. See comment. *Cancer Cell* **15,** 220–231
10. Yue, W. Y., and Chen, Z. P. (2005) Does vasculogenic mimicry exist in astrocytoma? *J. Histochem. Cytochem.* **53,** 997–1002
11. El Hallani, S., Boisselier, B., Peglion, F., Rousseau, A., Colin, C., Idbaih, A., Marie, Y., Mokhtari, K., Thomas, J. L., Eichmann, A., Delattre, J. Y., Maniotis, A. J., and Sanson, M. (2010) A new alternative mechanism in glioblastoma vascularization: tubular vasculogenic mimicry. *Brain* **133,** 973–982
12. Liu, X. M., Zhang, Q. P., Mu, Y. G., Zhang, X. H., Sai, K., Pang, J. C., Ng, H. K., and Chen, Z. P. (2011) Clinical significance of vasculogenic mimicry in human gliomas. *J. Neurooncol.* **105,** 173–179
13. Maniotis, A. J., Folberg, R., Hess, A., Seftor, E. A., Gardner, L. M., Pe'er, J., Trent, J. M., Meltzer, P. S., and Hendrix, M. J. (1999) Vascular channel formation by human melanoma cells *in vivo* and *in vitro*. Vasculogenic mimicry. *Am. J. Pathol.* **155,** 739–752
14. Folberg, R., and Maniotis, A.J. (2004) Vasculogenic mimicry. *Acta Pathol. Microbiol. Immunol. Scand.* **112,** 508–525
15. Ping, Y. F., and Bian, X. W. (2011) Concise review: Contribution of cancer stem cells to neovascularization. *Stem Cells* **29,** 888–894
16. Chen, Y., Jing, Z., Luo, C., Zhuang, M., Xia, J., Chen, Z., and Wang, Y. (2012) Vasculogenic mimicry-potential target for glioblastoma therapy. An *in vitro* and *in vivo* study. *Med. Oncol.* **29,** 324–331
17. Neufeld, G., Cohen, T., Gengrinovitch, S., and Poltorak, Z. (1999) Vascular endothelial growth factor (VEGF) and its receptors. *FASEB J.* **13,** 9–22
18. Yancopoulos, G. D., Klagsbrun, M., and Folkman, J. (1998) Vasculogenesis, angiogenesis, and growth factors. Ephrins enter the fray at the border. *Cell* **93,** 661–664
19. Eichmann, A., Corbel, C., Nataf, V., Vaigot, P., Bréant, C., and Le Douarin, N. M. (1997) Ligand-dependent development of the endothelial and hemopoietic lineages from embryonic mesodermal cells expressing vascular endothelial growth factor receptor 2. *Proc. Natl. Acad. Sci. U.S.A.* **94,** 5141–5146
20. Shalaby, F., Rossant, J., Yamaguchi, T. P., Gertsenstein, M., Wu, X. F., Breitman, M. L., and Schuh, A. C. (1995) Failure of blood-island formation and vasculogenesis in Flk-1-deficient mice. *Nature* **376,** 62–66
21. Fong, G. H., Rossant, J., Gertsenstein, M., and Breitman, M. L. (1995) Role of the Flt-1 receptor tyrosine kinase in regulating the assembly of vascular endothelium. *Nature* **376,** 66–70
22. Sun, J., Wang, D. A., Jain, R. K., Carie, A., Paquette, S., Ennis, E., Blaskovich, M. A., Baldini, L., Coppola, D., Hamilton, A. D., and Sebti, S. M. (2005) Inhibiting angiogenesis and tumorigenesis by a synthetic molecule that blocks binding of both VEGF and PDGF to their receptors. *Oncogene* **24,** 4701–4709
23. Yan, W., Bentley, B., and Shao, R. (2008) Distinct angiogenic mediators are required for basic fibroblast growth factor- and vascular endothelial growth factor-induced angiogenesis. The role of cytoplasmic tyrosine kinase c-Abl in tumor angiogenesis. *Mol. Biol. Cell* **19,** 2278–2288
24. Yamashita, J., Itoh, H., Hirashima, M., Ogawa, M., Nishikawa, S., Yurugi, T., Naito, M., Nakao, K., and Nishikawa, S. (2000) Flk1-positive cells derived from embryonic stem cells serve as vascular progenitors. *Nature* **408,** 92–96
25. Yang, L., Soonpaa, M. H., Adler, E. D., Roepke, T. K., Kattman, S. J., Kennedy, M., Henckaerts, E., Bonham, K., Abbott, G. W., Linden, R. M., Field, L. J., and Keller, G. M. (2008) Human cardiovascular progenitor cells develop from a KDR⁺ embryonic stem cell-derived population. *Nature* **453,** 524–528
26. Taura, D., Sone, M., Homma, K., Oyamada, N., Takahashi, K., Tamura, N., Yamanaka, S., and Nakao, K. (2009) Induction and isolation of vascular cells from human-induced pluripotent stem cells. Brief report. *Arterioscler. Thromb. Vasc. Biol.* **29,** 1100–1103
27. Shao, R., and Guo, X. (2004) Human microvascular endothelial cells immortalized with human telomerase catalytic protein. A model for the

study of *in vitro* angiogenesis. *Biochem. Biophys. Res. Commun.* **321,** 788–794

28. Francescone, R. A., 3rd, Faibish, M., and Shao, R. (2011) A Matrigel-based tube formation assay to assess the vasculogenic activity of tumor cells. *J. Vis. Exp.* **55,** 3040

29. Shao, R., Hamel, K., Petersen, L., Cao, Q. J., Arenas, R. B., Bigelow, C., Bentley, B., and Yan, W. (2009) YKL-40, a secreted glycoprotein, promotes tumor angiogenesis. *Oncogene* **28,** 4456–4468

30. Paik, J. H., Skoura, A., Chae, S. S., Cowan, A. E., Han, D. K., Proia, R. L., and Hla, T. (2004) Sphingosine 1-phosphate receptor regulation of N-cadherin mediates vascular stabilization. *Genes Dev.* **18,** 2392–2403

31. Luo, Y., High, F. A., Epstein, J. A., and Radice, G. L. (2006) N-cadherin is required for neural crest remodeling of the cardiac outflow tract. *Dev. Biol.* **299,** 517–528

32. Folkman, J. (1971) Tumor angiogenesis. Therapeutic implications. *N. Engl. J. Med.* **285,** 1182–1186

33. Hendrix, M.J., Seftor, E. A., Hess, A. R., and Seftor, R. E. (2003) Vasculogenic mimicry and tumor-cell plasticity. Lessons from melanoma. *Nat. Rev. Cancer* **3,** 411–421

34. Folberg, R., Arbieva, Z., Moses, J., Hayee, A., Sandal, T., Kadkol, S., Lin, A. Y., Valyi-Nagy, K., Setty, S., Leach, L., Chévez-Barrios, P., Larsen, P., Majumdar, D., Pe'er, J., and Maniotis, A. J. (2006) Tumor cell plasticity in uveal melanoma. Microenvironment directed dampening of the invasive and metastatic genotype and phenotype accompanies the generation of vasculogenic mimicry patterns. *Am. J. Pathol.* **169,** 1376–1389

35. di Tomaso, E., Capen, D., Haskell, A., Hart, J., Logie, J. J., Jain, R. K., McDonald, D. M., Jones, R., and Munn, L. L. (2005) Mosaic tumor vessels. Cellular basis and ultrastructure of focal regions lacking endothelial cell markers. *Cancer Res.* **65,** 5740–5749

36. Chang, Y. S., di Tomaso, E., McDonald, D. M., Jones, R., Jain, R. K., and Munn, L. L. (2000) Mosaic blood vessels in tumors. Frequency of cancer cells in contact with flowing blood. *Proc. Natl. Acad. Sci. U.S.A.* **97,** 14608–14613

37. Soda, Y., Marumoto, T., Friedmann-Morvinski, D., Soda, M., Liu, F., Michiue, H., Pastorino, S., Yang, M., Hoffman, R. M., Kesari, S., and Verma, I. M. (2011) Transdifferentiation of glioblastoma cells into vascular endothelial cells. *Proc. Natl. Acad. Sci. U.S.A.* **108,** 4274–4280

38. Wang, R., Chadalavada, K., Wilshire, J., Kowalik, U., Hovinga, K. E., Geber, A., Fligelman, B., Leversha, M., Brennan, C., and Tabar, V. (2010) Glioblastoma stem-like cells give rise to tumor endothelium. *Nature* **468,** 829–833

39. Ricci-Vitiani, L., Pallini, R., Biffoni, M., Todaro, M., Invernici, G., Cenci, T., Maira, G., Parati, E. A., Stassi, G., Larocca, L. M., and De Maria, R. (2010) Tumor vascularization via endothelial differentiation of glioblastoma stem-like cells. *Nature* **468,** 824–828

40. Döme, B., Hendrix, M.J., Paku, S., Tóvári, J., and Tímár, J. (2007) Alternative vascularization mechanisms in cancer. Pathology and therapeutic implications. *Am. J. Pathol.* **170,** 1–15

41. Folberg, R., Hendrix, M. J., and Maniotis, A. J. (2000) Vasculogenic mimicry and tumor angiogenesis. *Am. J. Pathol.* **156,** 361–381

42. Wurmser, A. E., Nakashima, K., Summers, R. G., Toni, N., D'Amour, K. A., Lie, D. C., and Gage, F. H. (2004) Cell fusion-independent differentiation of neural stem cells to the endothelial lineage. *Nature* **430,** 350–356

43. Eliceiri, B. P. (2001) Integrin and growth factor receptor cross-talk. *Circ. Res.* **89,** 1104–1110

44. Wijelath, E. S., Murray, J., Rahman, S., Patel, Y., Ishida, A., Strand, K., Aziz, S., Cardona, C., Hammond, W. P., Savidge, G. F., Rafii, S., and Sobel, M. (2002) Novel vascular endothelial growth factor binding domains of fibronectin enhance vascular endothelial growth factor biological activity. *Circ. Res.* **91,** 25–31

45. Borges, E., Jan, Y., and Ruoslahti, E. (2000) Platelet-derived growth factor receptor β and vascular endothelial growth factor receptor 2 bind to the β3 integrin through its extracellular domain. *J. Biol. Chem.* **275,** 39867–39873

46. Miller, K., Wang, M., Gralow, J., Dickler, M., Cobleigh, M., Perez, E. A., Shenkier, T., Cella, D., and Davidson, N. E. (2007) Paclitaxel plus bevacizumab *versus* paclitaxel alone for metastatic breast cancer. *N. Engl. J. Med.* **357,** 2666–2676

47. Hurwitz, H., Fehrenbacher, L., Novotny, W., Cartwright, T., Hainsworth, J., Heim, W., Berlin, J., Baron, A., Griffing, S., Holmgren, E., Ferrara, N., Fyfe, G., Rogers, B., Ross, R., and Kabbinavar, F. (2004) Bevacizumab plus irinotecan, fluorouracil, and leucovorin for metastatic colorectal cancer. See comment. *N. Engl. J. Med.* **350,** 2335–2342

48. Sandler, A., Gray, R., Perry, M. C., Brahmer, J., Schiller, J. H., Dowlati, A., Lilenbaum, R., and Johnson, D. H. (2006) Paclitaxel-carboplatin alone or with bevacizumab for non-small-cell lung cancer. *N. Engl. J. Med.* **355,** 2542–2550

49. Manegold, C. (2008) Bevacizumab for the treatment of advanced non-small cell lung cancer. *Expert Rev. Anticancer Ther.* **8,** 689–699

50. Norden, A. D., Young, G. S., Setayesh, K., Muzikansky, A., Klufas, R., Ross, G. L., Ciampa, A. S., Ebbeling, L. G., Levy, B., Drappatz, J., Kesari, S., and Wen, P. Y. (2008) Bevacizumab for recurrent malignant gliomas. Efficacy, toxicity, and patterns of recurrence. *Neurology* **70,** 779–787

51. Mancuso, M. R., Davis, R., Norberg, S. M., O'Brien, S., Sennino, B., Nakahara, T., Yao, V. J., Inai, T., Brooks, P., Freimark, B., Shalinsky, D. R., Hu-Lowe, D. D., and McDonald, D. M. (2006) Rapid vascular regrowth in tumors after reversal of VEGF inhibition. *J. Clin. Invest.* **116,** 2610–2621

52. Keunen, O., Johansson, M., Oudin, A., Sanzey, M., Rahim, S. A., Fack, F., Thorsen, F., Taxt, T., Bartos, M., Jirik, R., Miletic, H., Wang, J., Stieber, D., Stuhr, L., Moen, I., Rygh, C. B., Bjerkvig, R., and Niclou, S. P. (2011) Anti-VEGF treatment reduces blood supply and increases tumor cell invasion in glioblastoma. *Proc. Natl. Acad. Sci. U.S.A.* **108,** 3749–3754

53. Batchelor, T. T., Sorensen, A. G., di Tomaso, E., Zhang, W. T., Duda, D. G., Cohen, K. S., Kozak, K. R., Cahill, D. P., Chen, P. J., Zhu, M., Ancukiewicz, M., Mrugala, M. M., Plotkin, S., Drappatz, J., Louis, D. N., Ivy, P., Scadden, D. T., Benner, T., Loeffler, J. S., Wen, P. Y., and Jain, R. K. (2007) AZD2171, a pan-VEGF receptor tyrosine kinase inhibitor, normalizes tumor vasculature and alleviates edema in glioblastoma patients. *Cancer Cell* **11,** 83–95

54. Kamoun, W. S., Ley, C. D., Farrar, C. T., Duyverman, A. M., Lahdenranta, J., Lacorre, D. A., Batchelor, T. T., di Tomaso, E., Duda, D. G., Munn, L. L., Fukumura, D., Sorensen, A. G., and Jain, R. K. (2009) Edema control by cediranib, a vascular endothelial growth factor receptor-targeted kinase inhibitor, prolongs survival despite persistent brain tumor growth in mice. *J. Clin. Oncol.* **27,** 2542–2552

55. Winkler, F., Kozin, S. V., Tong, R. T., Chae, S. S., Booth, M. F., Garkavtsev, I., Xu, L., Hicklin, D. J., Fukumura, D., di Tomaso, E., Munn, L. L., and Jain, R. K. (2004) Kinetics of vascular normalization by VEGFR2 blockade governs brain tumor response to radiation. Role of oxygenation, angiopoietin-1, and matrix metalloproteinases. *Cancer Cell* **6,** 553–563

56. Timke, C., Zieher, H., Roth, A., Hauser, K., Lipson, K. E., Weber, K. J., Debus, J., Abdollahi, A., and Huber, P. E. (2008) Combination of vascular endothelial growth factor receptor/platelet-derived growth factor receptor inhibition markedly improves radiation tumor therapy. *Clin. Cancer Res.* **14,** 2210–2219

57. Kozin, S. V., Boucher, Y., Hicklin, D. J., Bohlen, P., Jain, R. K., and Suit, H. D. (2001) Vascular endothelial growth factor receptor-2-blocking antibody potentiates radiation-induced long term control of human tumor xenografts. *Cancer Res.* **61,** 39–44

58. Lee, J., Kotliarova, S., Kotliarov, Y., Li, A., Su, Q., Donin, N. M., Pastorino, S., Purow, B. W., Christopher, N., Zhang, W., Park, J. K., and Fine, H. A. (2006) Tumor stem cells derived from glioblastomas cultured in bFGF and EGF more closely mirror the phenotype and genotype of primary tumors than do serum-cultured cell lines. *Cancer Cell* **9,** 391–403

59. Basu, G. D., Liang, W. S., Stephan, D. A., Wegener, L. T., Conley, C. R., Pockaj, B. A., and Mukherjee, P. (2006) A novel role for cyclooxygenase-2 in regulating vascular channel formation by human breast cancer cells. *Breast Cancer Res.* **8,** R69

60. Liu, C., Huang, H., Doñate, F., Dickinson, C., Santucci, R., El-Sheikh, A., Vessella, R., and Edgington, T. S. (2002) Prostate-specific membrane antigen-directed selective thrombotic infarction of tumors. *Cancer Res.* **62,** 5470–5475

61. Sood, A. K., Fletcher, M. S., Zahn, C. M., Gruman, L. M., Coffin, J. E., Seftor, E. A., and Hendrix, M. J. (2002) The clinical significance of tumor cell-lined vasculature in ovarian carcinoma. Implications for anti-vasculogenic therapy. *Canc. Biol. Ther.* **1,** 661–664